RESEARCH ARTICLE | *Fluid and Electrolyte Homeostasis*

Functional characterization and osmoregulatory role of the Na^+-K^+-$2Cl^-$ cotransporter in the gill of sea lamprey (*Petromyzon marinus*), a basal vertebrate

 Ciaran A. Shaughnessy[1] and Stephen D. McCormick[2,3]

[1]*Graduate Program in Organismic and Evolutionary Biology, University of Massachusetts, Amherst, Massachusetts;*
[2]*United States.Geological Survey, Leetown Science Center, Conte Anadromous Fish Research Laboratory, Turners Falls, Massachusetts; and* [3]*Department of Biology, University of Massachusetts, Amherst, Massachusetts*

Shaughnessy CA, McCormick SD. Functional characterization and osmoregulatory role of the Na^+-K^+-$2Cl^-$ cotransporter in the gill of sea lamprey (*Petromyzon marinus*), a basal vertebrate. *Am J Physiol Regul Integr Comp Physiol* 318: R17–R29, 2020. First published October 16, 2019; doi:10.1152/ajpregu.00125.2019.—The present study provides molecular and functional characterization of Na^+-K^+-$2Cl^-$ cotransporter (NKCC1/Slc12a2) in the gills of sea lamprey (*Petromyzon marinus*), the most basal extant vertebrate with an osmoregulatory strategy. We report the full-length peptide sequence for the lamprey Na-K-Cl cotransporter 1 (NKCC1), which we show groups strongly with and occupies a basal position among vertebrate NKCC1 sequences. In postmetamorphic juvenile lamprey, *nkcc1* mRNA was present in many tissues but was fivefold higher in the gill than any other examined tissue, and NKCC1 protein was only detected in the gill. Gill mRNA and protein abundances of NKCC1 and Na^+-K^+-ATPase (NKA/Atp1a1) were significantly upregulated (20- to 200-fold) during late metamorphosis in fresh water, coinciding with the development of salinity tolerance, and were upregulated an additional twofold after acclimation to seawater (SW). Immunohistochemistry revealed that NKCC1 in the gill is found in filamental ionocytes coexpressing NKA, which develop during metamorphosis in preparation for SW entry. Lamprey treated with bumetanide, a widely used pharmacological inhibitor of NKCC1, exhibited higher plasma Cl^- and osmolality as well as reduced muscle water content after 24 h in SW; there were no effects of bumetanide in freshwater-acclimated lamprey. This work provides the first functional characterization of NKCC1 as a mechanism for branchial salt secretion in lampreys, providing evidence that this mode of Cl^- secretion has been present among vertebrates for ~550 million years.

ion regulation; metamorphosis; osmoregulation

INTRODUCTION

The Na^+-K^+-$2Cl^-$ cotransporter 1 (NKCC1/Slc12a2) belongs to the SLC12A family of electroneutral cation-chloride cotransporters, which includes two Na-K-Cl cotransporter (NKCC) isoforms (NKCC1 and NKCC2/Slc12a1), Na^+-Cl^- cotransporter (NCC/Slc12a2), and K^+-Cl^- cotransporters (KCC[1–3]/Slc12a[4–6]). NKCCs are responsible for the inward movements of Na^+, K^+, and Cl^- across the cell membrane with a $1Na^+$:$1K^+$:$2Cl^-$ stoichiometry and are involved in a wide variety of physiological processes, including electrolyte and fluid homeostasis and regulation of blood pressure, pain perception, and neuronal signaling (19, 33, 55). Although the two isoforms of NKCC have high sequence similarity, they are easily distinguished by their distribution throughout the body and roles in ion transport. The basolateral NKCC1 is distributed throughout the vertebrate body, contributing to cell volume regulation, and is highly expressed in ion-secreting epithelia and some other nonepithelial tissues, such as immature neurons (19, 33, 55). The absorptive, apically located NKCC2 is expressed in the kidneys and intestines of mammals and fishes (8, 13, 35, 45, 69). The importance and relevance of NKCC1 is highlighted by extensive pharmacological and genetic work targeting NKCC1, with multiple loop diuretics (primarily bumetanide and furosemide) (58) and links between NKCC1 dysfunction and hypertension and neurological disorders, such as epilepsy (29). Early work that characterized NKCC in mammalian cells first described a coupled transport of Na^+ and K^+ (65) and then the coordinated cotransport of Cl^- (18). A cDNA-encoding NKCC1 was first cloned, and its ionoregulatory role in the shark rectal gland was described (36, 68). Since these early works, NKCC1 has been shown to be a conserved basolateral pathway in epithelial Cl^- secretion, appearing within Cl^- secreting cell types of the mammalian lung and colon, shark rectal gland, reptilian/avian salt gland, and fish gill (20).

Lampreys (Petromyzontiformes) are one of two extant members, along with the hagfishes (Myxiniformes), of the phylogenetically ancient group of jawless vertebrates known as cyclostomes, which make up the superclass Agnatha. Genomic analysis indicates that Petromyzontiformes may have radiated more than 550 million years ago (61). Unlike hagfish, which do not regulate their internal osmotic concentration, lampreys maintain an internal osmolality of approximately one-third that of seawater (SW), an osmoregulatory strategy shared among nearly every other vertebrate species (6). Thus, lampreys represent the most basal extant order of osmoregulating vertebrates and are therefore an important group for understanding the evolution of osmoregulatory mechanisms.

Sea lamprey (*Petromyzon marinus*, Linnaeus 1758) are anadromous, making a freshwater (FW)-to-SW migration as juveniles to access more abundant food resources in the ocean before returning upstream years later as mature adults to spawn. The general life history of anadromous lampreys is well

Address for reprint requests and other correspondence: C. A. Shaughnessy, Conte Anadromous Fish Research Laboratory, 1 Migratory Way, Turners Falls, MA 01376 (e-mail: cshaughnessy@umass.edu).

described (3, 49, 73), including a FW-resident, filter-feeding larval stage and a true metamorphosis to a juvenile stage, which is characterized into seven intermediary stages between larvae and postmetamorphic juveniles primarily based on development of the eye and parasitic mouth structure (70, 71). Physiological changes that accompany metamorphosis include an increase in gill Na^+-K^+-ATPase (NKA) activity and protein abundance (52), an increase in abundance of ionocytes, and the development of SW tolerance (4, 54). It is not until after metamorphosis is complete and SW tolerance has developed that juvenile anadromous lampreys migrate to the sea.

To maintain internal osmotic and ionic homeostasis, jawless and bony fishes entering SW must absorb water and secrete ions against steep gradients between their internal fluids and the more concentrated marine environment. This is accomplished by a coordinated process of drinking SW, actively desalinating and absorbing water across gastrointestinal epithelia, and secreting ions (primarily Na^+ and Cl^-) across the branchial epithelium (37). The cellular mechanism for epithelial Na^+ and Cl^- secretion in teleosts, elasmobranchs, and tetrapods is highly conserved and primarily involves three membrane-bound ion transporters: NKA, NKCC1, and a cystic fibrosis transmembrane conductance regulator (CFTR/Abcc7) chloride channel. Activity of NKA and the presence of an inward-rectifying K^+ channel on the basolateral membrane of Cl^--secreting, mitochondrion-rich ionocytes (classically referred to as "chloride cells") are responsible for producing *1*) the sodium gradient that drives Na^+-coupled transport of Cl^- from the extracellular compartment into the cell via the basolateral NKCC1, as well as *2*) the inside-negative resting membrane potential that facilitates secretion of Cl^- out of the cell through the apical CFTR). In fish, upregulation of NKA, NKCC1, and CFTR in the gill is a general response to elevated salinity. Some anadromous fishes, such as Atlantic salmon (*Salmo salar*), upregulate gill NKA, NKCC1, and CFTR in anticipation of the hypo-osmoregulatory requirements of SW before they ever experience an increase in salinity (40, 41).

The mechanism for branchial Cl^- section among the most basal osmoregulating fishes, i.e., sturgeons and lampreys, is not well described. It has been shown in sturgeon that gill NKCC1 and NKA may have a role in hypo-osmoregulation in SW (56, 59). In sea lamprey, it has been demonstrated that a basolateral NKA is important in branchial ion transport in FW and SW (15, 52) and that gill *nkcc1* mRNA abundance in upstream-migrating adults was observed to increase after transfer from FW back to SW (15). No work has been done to link the development of hypo-osmoregulatory ability to specific molecular mechanisms for Cl^- secretion (i.e., basolateral NKCC1 or apical CFTR) in the basal lampreys, and no protein- or organism-level evidence exists demonstrating a functional role of NKCC1 in ion regulation or SW tolerance in lamprey. Here, we present a functional characterization of the role and regulation of NKCC1 in the Cl^--secreting ionocytes of the sea lamprey, an extant representative of the most basal vertebrate clade.

MATERIALS AND METHODS

Experimentation and tissue collection. The experiments in this study were performed in accordance with protocols approved by the Institutional Animal Care and Use Committees at the University of Massachusetts (protocol no. 2016–0009). Sea lamprey used in this study were captured from the Connecticut River watershed in Massachusetts, and all experiments were performed at the S.O. Conte Anadromous Fish Research Center (Leetown Science Center, United States Geological Survey) in Turners Falls, MA. Lamprey held in the laboratory were kept at ambient temperature under a natural photoperiod in 1.5-m diameter flow-through tanks with 10-cm deep sandy substrate for burrowing and were supplied with aerated, filtered, and UV-treated Connecticut River water. All laboratory experimentation was carried out at 15°C under a simulated natural photoperiod in 60-L recirculating aquarium tanks supplied with dechlorinated municipal water and equipped with mechanical, biological, and chemical filtration. Artificial SW (35 ‰) was made by dissolving an artificial sea salt mix (Crystal Sea Salt, Baltimore, MD) in dechlorinated municipal water.

The salinity tolerance of larvae and various stages throughout metamorphosis was tested by gradually (in the case of larvae) or directly exposing lamprey to elevated salinity and assessing survival. Tissue profile samples were collected from postmetamorphic juveniles acclimated to FW. Gill tissue for the metamorphic profile was obtained from lamprey immediately after capture via electrofishing (Stage 7 larvae) or Fyke netting (downstream-running "migrants") in the Sawmill River (Montague, MA) from July to November. Gill tissue for the larval FW to SW comparison was collected from larvae and postmetamorphic juveniles in FW or those acclimated to SW for 3 wk. Pharmacological inhibition experiments were conducted with postmetamorphic juveniles acclimated to FW. Lamprey were anesthetized in a nonlethal dose of tricaine mesylate (100 mg/L buffered with $NaHCO_3$, pH 7.0) and administered via intraperitoneal injection using a 25-gauge needle a 20 μL/g volume of sterile-filtered saline (0.9% NaCl) containing one of two doses of bumetanide (1.0 or 0.1 μmol/g) or a vehicle control (VEH). Lamprey recovered within minutes after anesthetization and were allowed an additional 30–60 min of recovery in FW after injection and then placed in 35 ‰ SW or a FW control and sampled for blood and tissue 24 h later.

For all field and laboratory tissue collection, lamprey were euthanized using a lethal dose of tricaine mesylate (200 mg/L). Blood was collected into capillary tubes from the caudal vasculature, and plasma was separated via centrifugation. Plasma and tissues were immediately collected, then frozen and stored at −80°C. Plasma Cl^- was measured using a digital chloridometer (Haake Buchler Instruments Inc., Saddlebrook, NJ), and plasma osmolality was measured using a vapor pressure osmometer (Wescor, Logan, UT). For muscle water analysis, 0.1–0.2 g of white muscle was blotted dry and weighed (wet mass) then placed in a drying oven for 48 h at 60°C until dehydrated to a stable weight (dry mass).

Sequence assembly and phylogenetic analysis of lamprey nkcc1. A partial sequence (one-third of the total length) of the sea lamprey *nkcc1* gene containing the 3′ end was identified in the sea lamprey genome assembly (62). To obtain a full-length sequence of the gene, rapid amplification of cDNA ends (RACE) was performed. Total RNA (1 μg) was isolated from the gills of three postmetamorphic juveniles and reverse transcribed using the SMARTer RACE cDNA Amplification Kit (Takara Bio USA, Palo Alto, CA) following the manufacturer's protocol. Polymerase chain reaction (PCR) products between an antisense gene-specific primer (5′-CGC TCA CGA GTA GAA CGT CA-3′) and a proprietary universal primer were confirmed electrophoretically on a 1% agarose gel, then extracted and purified using the UltraClean GelSpin DNA Extraction Kit (MoBio, Solana Beach, CA) and then commercially sequenced (GENEWIZ, South Plainfield, NJ). A complete cDNA sequence including 5′ and 3′ untranslated regions was assembled by appending RACE-obtained 5′ *nkcc1* sequences with the partial 5′ and 3′ sequences available in the sea lamprey genome assembly and verified by sequencing products of long-range PCR reactions (KAPA Long Range DNA Polymerase, Kapa Biosystems, Wilmington, MA) spanning between primers at the

5′ end (5′-ACA GAG GAA CGG GAG AAG CG-3′) and 3′ end (5′-CGC TCA CGA GTA GAA CGT CA-3′).

An amino acid sequence for the sea lamprey NKCC1 gene was deduced from the obtained *nkcc1* cDNA sequence, and its molecular mass was predicted using the Translate and TrEMBL tools, respectively, provided by the ExPASy bioinformatics resource portal (https://www.expasy.org). Hypothetical membrane topology and potential *N*-linked glycosylation sites were predicted using the TMHMM and NetNGlyc tools, respectively, provided by DTU Bioinformatics server (https://www.bioinformatics.dtu.dk). Phylogenetic analysis was carried out on a balanced selection of vertebrate NKCC1, NKCC2, and NCC (NCC1) peptides available from NCBI GenBank using a ClustalW alignment (https://www.ebi.ac.uk/clustalw) and the Neighbor-Joining method (1,000 bootstrap replicates) implemented by MEGA7 software (32). Accession numbers for the peptides used in the phylogenetic analysis were Ghostshark NKCC1 (XP_007890727), Ghostshark NCC (XP_007905777), Salmon NKCC1 (XP_020313370), Salmon NCC (XP_020311909), Zebrafish NKCC1 (NP_001002080), Zebrafish NKCC2 (XP_009291678), Zebrafish NCC (NP_001038545), Frog NKCC1 (XP_004910530), Frog NKCC2 (XP_012814934), Frog NCC (XP_002937217), Chicken NKCC1 (XP_003643107), Chicken NKCC2 (XP_004943856), Chicken NCC (XP_015134720), Mouse NKCC1 (NP_033220), Mouse NKCC2 (NP_001073158), Mouse NCC (NP_001192240), Human NKCC1 (NP_001243390), Human NKCC2 (NP_000329), Human NCC (NP_000330), and Human KCC1 (AAH21193.1).

Quantitative real-time polymerase chain reaction. Total RNA was isolated from frozen tissue using TRIzol reagent (Molecular Research Center Inc., Cincinnati, OH) following the manufacturer's protocol. Total RNA concentration and purity of each sample was determined spectrophotometrically using a Take3 microvolume plate (BioTek Instruments, Winooski, VT), and RNA integrity was assessed using gel electrophoresis. Only high-purity ($1.9 <$ A260 and A280 > 2.2) and high-integrity RNA samples were used for cDNA synthesis. First-strand cDNA synthesis was accomplished using the High-Capacity Reverse Transcription Kit (Applied Biosystems, Carlsbad, CA) following the manufacturer's protocol. Quantitative real-time PCR (qPCR) was carried out in 10 μL reactions containing 2 ng cDNA template, 200 nM forward and reverse primers, and SYBRSelect master mix (Thermo Fisher Scientific, Waltham, MA). Primer pairs were identical to those already reported for *nkcc1* and *nka* (15) and *ef1α* (31). Four potential reference genes were analyzed: *gapdh*, *18s*, *β-actin*, and *ef1α*. The reference gene *ef1α* was determined to be stable ($\pm$ 1 cycle threshold) across all metamorphic and life stages, tissues, and salinities for the analyses presented. All qPCR reactions were performed in optical 96-well reaction plates in a StepOnePlus Real-Time PCR System (Applied Biosystems, Foster City, CA) using the following thermal profile: holding at 50°C (2 min), then activation at 95°C (2 min); cycling (40 cycles) from 95°C (15 s) to 60°C (1 min) to 72°C (30 s). A single product was confirmed for every reaction via a dissociation step (melt curve analysis) increasing from 60°C to 95°C after the cycling protocol, and for each primer pair electrophoretically.

Immunoblotting. Gill tissue was homogenized in SEID buffer (150 mmol/L sucrose, 10 mmol/L EDTA, 50 mmol/L imidazole, and 0.1% sodium deoxycholate, pH 7.3) and centrifuged at 2,000 *g* for 5 min, and the supernatant was used for protein abundance quantification by Western blot analysis. The supernatant was analyzed for protein content using the Pierce BCA Protein Assay (Thermo Fisher Scientific, Rockford, IL) and diluted in Laemmli sample buffer, denatured by heating for 15 min at 60°C, and stored at −80°C. For subcellular fractionation, before diluting in Laemmli buffer, the supernatant was first centrifuged again at 48,000 *g* for 1 h; the resulting supernatant was considered "cytosol," and the pellet (resuspended in SEID) was considered "membrane." Samples were run at 5 μg protein per lane along with a Precision Plus protein standard for size reference on a 7.5% sodium dodecyl sulfate polyacrylamide gel electrophoresis minigel (Bio-Rad, Hercules, CA) for electrophoretic separation, and then transferred to

Immobilon polyvinylidene fluoride (PVDF) transfer membranes (Millipore, Bedford, MA). After transfer, the PVDF membranes were dried and stored overnight at room temperature. PVDF membranes were rehydrated in methanol, then equilibrated to phosphate-buffered saline with 0.05% Triton X-100 (PBST), blocked for 1 h at 23°C in 5% nonfat milk in PBST, and finally incubated overnight at 4°C in a 1:4,000 dilution of primary antibody (Developmental Studies Hybridoma Ban, Iowa City, IA): mouse monoclonal anti-NKA α-subunit ["α5"; Research Resource Identifier (RRID): AB_2166869], mouse monoclonal anti-NKCC/NCC ('T4', RRID: AB_528406), mouse monoclonal anti-NKCC ("T9", RRID: AB_2618107), or mouse monoclonal anti-HSP90 ("H90", RRID: AB_2051648). After primary incubation, membranes were washed with PBST and then incubated for 2 h at 23°C in a 1:10,000 dilution of the horseradish peroxidase-conjugated goat anti-mouse secondary antibody (Kirkegaard & Perry Laboratories, Gaithersburg, MA) in blocking buffer. After secondary antibody incubation, membranes were washed with PBST and imaged by a Syngene PXi system (SYNGENE, Frederick, MD) via enhanced chemiluminescence (ECL) using a 1:1 mixture of ECL solution A (396 μmol/L coumaric acid, 2.5 mmol/L luminol, 100 mmol/L Tris·HCl, pH 8.5) and ECL solution B (0.018% H_2O_2, 100 mmol/L Tris·HCl, pH 8.5). Band intensity was measured using ImageJ (National Institutes of Health, Bethesda, MD). The use of α5 and T9 antibodies was validated for use in Western blotting as follows: *1*) a specific band was present at an expected molecular weight for each protein, *2*) a linear relationship was observed between band intensity and the amount of protein sample loaded into each well (0.1 to 20 μg), and *3*) no evidence of false positive or nonspecific binding was observed in 3 different negative controls: gill protein incubated with no primary antibody (secondary only) ([−]Ab), gill protein incubated with a primary antibody produced under the same conditions ([+]T4), and protein from tissues expected to have only very low NKCC1 abundance (i.e., matching mRNA and protein tissue profiles). Our lower detection limit for T9 and α5 immunoreactivity in Western blotting, using a pool of SW-acclimated juveniles, was ~0.12 and 0.11 μg/lane, which correspond to 1/42 and 1/47 the amount loaded in our Western blotting protocol (5 μg/lane). Undetected bands during quantification were assigned the lower limit of detection, and protein abundance is expressed as relative to the lower limit of detection (undetected bands = 1). Identical pooled samples were run on each gel and used as a calibrator to correct for any interblot variation.

Immunohistochemistry. Whole gill pouches were fixed in 4% paraformaldehyde in 10 mM phosphate-buffered saline (PBS) at room temperature for 2 h, then preserved in 70% ethanol. Before sectioning, gill tissue was rinsed in PBS, equilibrated to 30% (wt/vol) sucrose in PBS, and then frozen in embedding medium (TissueTek, Sakura Finetek, Torrance, CA). Embedded gill tissue was sectioned (5 μm thick) at −20°C, electrostatically mounted to microscope slides (Fisherbrand Colorfrost Plus, Fisher Scientific, Hampton, NH), and then dried at room temperature to ensure adherence to the slide. Before incubation with primary antibody, mounted gill tissue was rehydrated in PBS, incubated for 30 min in 0.3% (wt/vol) Sudan Black B to reduce autofluorescence, and then incubated for 30 min in a blocking solution (10% normal goat serum in PBS). Slides were incubated overnight at 4°C in primary antibody [T4, 1:1,000 (negative control only); T9, 1:1,000] in antibody dilution buffer (0.01% NaN₃, 0.1% bovine serum albumin, 2% normal goat serum, and 0.02% keyhole limpet hemocyanin in PBS). For colocalization, slides were coincubated with T9 and a rabbit monoclonal anti-NKA primary antibody (αRbNKA, 1:1,000) (66). After primary incubation, slides were washed in PBS and then incubated for 2 h at room temperature in fluorescently labeled secondary antibody (goat anti-mouse, Alexa 546) diluted 1:1,000 in antibody dilution buffer. After secondary incubation, slides were again washed in PBS, covered with a cover-
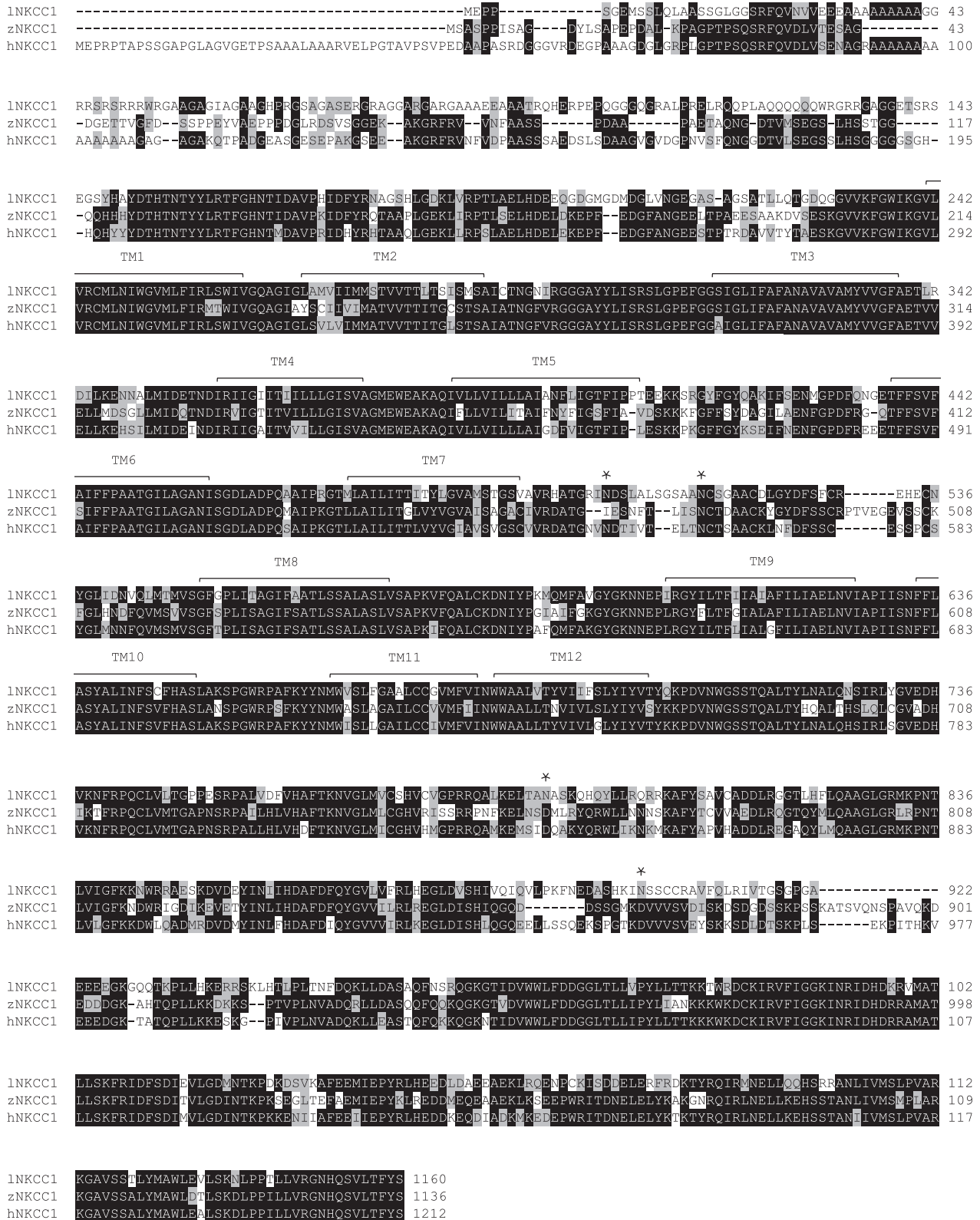
Fig. 1. Multiple alignments of peptide sequence for the Na-K-Cl cotransporter 1 (NKCC1) of zebrafish (zNKCC1) and humans (hNKCC1) and the deduced amino acid sequence for sea lamprey *nkcc1* (lNKCC1). Black shading indicates identical residues and gray shading indicates chemically similar residues. Horizontal bars indicate the 12 predicted transmembrane segments. *Predicted N-linked glycosylation sites.

slip, and examined with a Nikon Diaphot-TMD inverted fluorescence microscope (×20) with a mercury lamp. Validation of T9 use in immunohistochemistry was similar to our validations used in Western blotting. Negative control validation included the absence of signal in *1*) gill sections incubated with secondary antibody only, *2*) gill sections incubated with T4, and *3*) sections of nontarget tissues incubated with T9. T9-immunoreactive cells on the primary filament or secondary lamellae were tallied from unique sections (3–5 sections per individual) from larvae, FW-acclimated juveniles, and SW-acclimated juveniles (*n* = 5 per group).

Calculations and statistical analyses. Muscle moisture (%) was calculated as [(wet mass − dry mass) × 100]/wet mass. Shapiro-Wilk and Levene's tests were used to test assumptions of normality and homogeneity, respectively. Significant differences between treatments were analyzed using one-way or two-way ANOVA analyses and were identified by Dunn's post hoc (all Western blot and immunohistochemistry data) or Student-Newman-Keuls post hoc analyses (all other data). An α value of 0.05 was selected to denote statistical significance in all analyses. Relative protein abundances of juvenile gill NKCC1 and NKA were regressed, and the correlation was assessed by calculating the slope (*m*), coefficient of determination (r^2), and significance. Statistics and figures were completed using R statistical software version 3.2.2 (https://www.r-project.org) and GraphPad Prism 6.0 (GraphPad Software, La Jolla, CA).

RESULTS

Molecular characterization and tissue profile of NKCC1. We obtained a sequence for the sea lamprey *nkcc1* gene that comprised 3,480 bp coding for a mature NKCC1 peptide sequence of 1,160 amino acids with a predicted molecular mass of 127 kDa (NCBI GenBank accession no. MK779970). The sea lamprey NKCC1 has a 66% sequence identity with the NKCC1 of both zebrafish (*Danio rerio*) and human (*Homo sapiens*), which have a 72% sequence identity with each other (Fig. 1). Phylogenetic analysis of other vertebrate cation-chloride cotransporters placed the sea lamprey NKCC1 at the basal position in a clade with other vertebrate NKCC1 peptides, which was distinct from clades of vertebrate NKCC2 or NCC peptides (Fig. 2). In Western blotting, no banding was detected using the T4 antibody, but probing with T9 reliably detected a single, diffuse immunoreactive band centered around an approximate molecular mass of 180 kDa, which appeared to be most intense in SW-acclimated juveniles (Fig. 3*A*). T9 immunoreactivity was only detected in the membrane fraction of a gill homogenate from FW- or SW-acclimated juveniles, whereas HSP90 (90 kDa) was mostly detected in the cytosolic fraction (Fig. 3*B*). In tissue profiles, mRNA abundance of *nkcc1* was at least fivefold higher in the gill of an FW-acclimated sea lamprey than in any other tissue examined (Fig. 3*C*), and T9-immunoreactivity (NKCC1 protein) was only detected in the gill (Fig. 3*D*).

Salinity tolerance. Larvae serving as an FW control all survived (Fig. 4*A*). During exposure to increasing salinity, larval mortality first occurred in 10‰ and all larvae died between 10‰ and 15‰ (Fig. 4*A*). Exposure to 10‰ for 14 d resulted in 0% survival in larvae and 30% survival in metamorphic stages 2–5 (Fig. 4*B*). Survival in 25‰ was 0% in larvae and early metamorphic stages 2–5 and then increased dramatically to over 95% in stages 6–7 and 100% in postmetamorphic juveniles (Fig. 4*B*).

Metamorphic profile of NKCC1 and effect of SW acclimation. In gill tissue collected from wild sea lamprey at various stages of metamorphosis, *nkcc1* mRNA increased 200-fold from larvae to postmetamorphic downstream migrants ($P < 0.001$; Fig. 5*A*), and NKCC1 protein abundance increased at least 25-fold from larvae (undetected) to migrants ($P < 0.001$; Fig. 5*B*). Similarly, gill *nka* increased 15-fold throughout metamorphosis ($P < 0.001$; Fig. 5*C*) and gill NKA protein
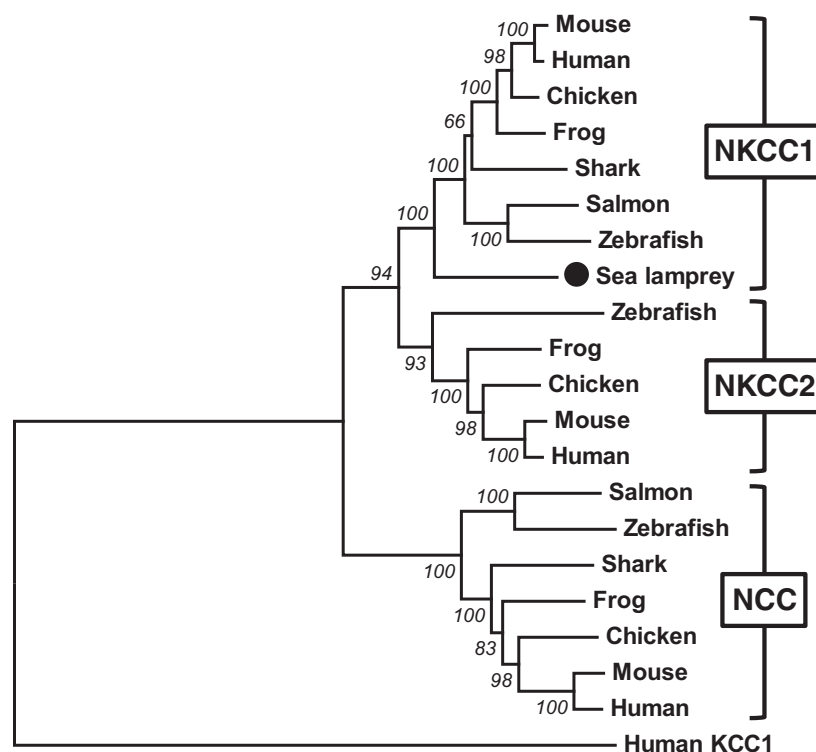

Fig. 2. Phylogeny of the coding regions of various vertebrate cation-chloride cotransporters [Na-K-Cl cotransporter (NKCC) 1, NKCC2, and Na^+-Cl^- cotransporter (NCC), with a human K^+-Cl^- cotransporter (KCC1) outgroup] constructed using the Neighbor-Joining method with 1,000 replicates. Sea lamprey NKCC1 is highlighted by a filled circle.
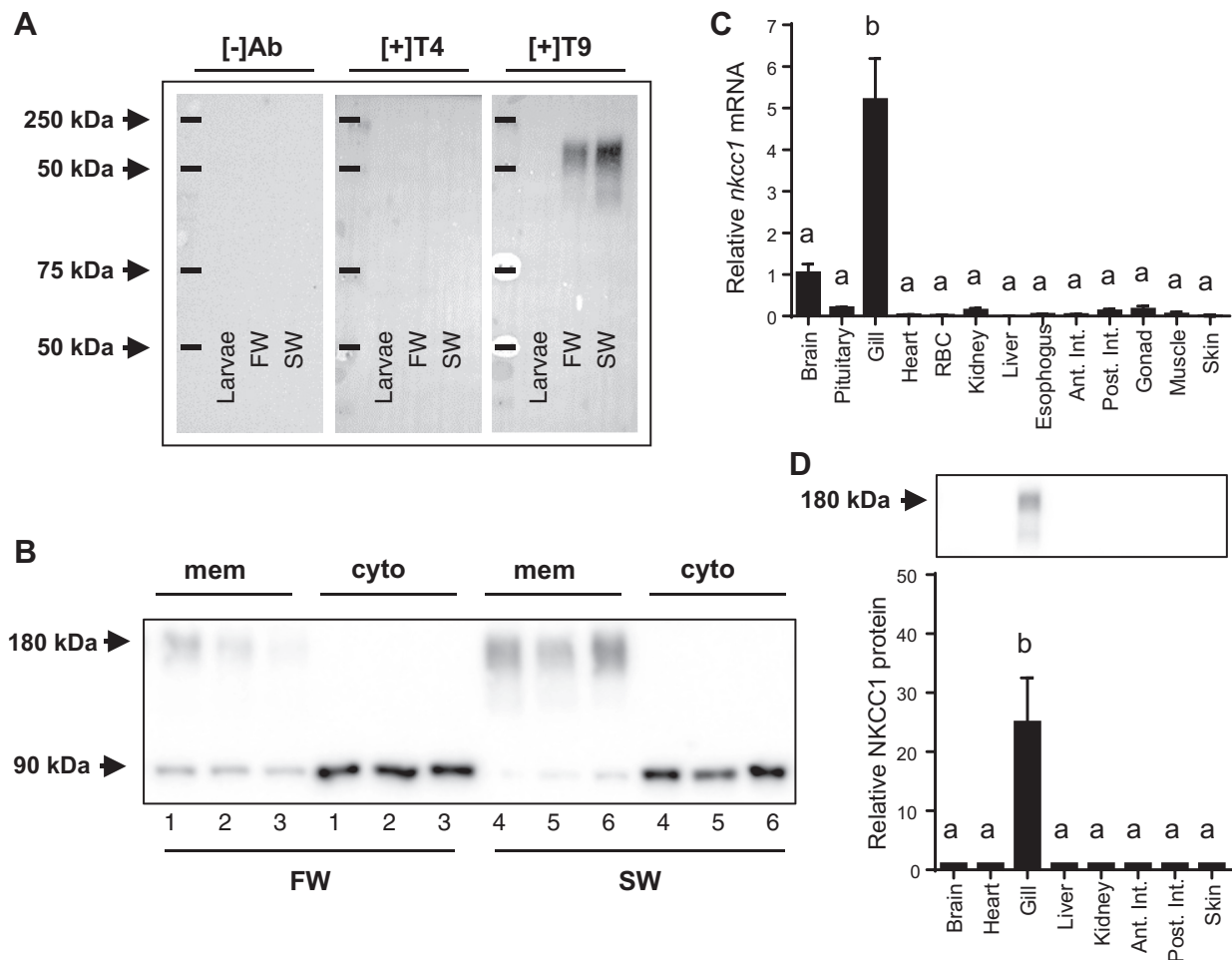
Fig. 3. Validation blots showing T9-specific immunoreactive banding (~180 kDa) (*A*) and Na-K-Cl cotransporter 1 (NKCC1) subcellular location (*B*) as well as tissue profiles for the relative abundance of *nkcc1* mRNA (*C*) and NKCC1 protein (*D*) in freshwater (FW)-acclimated juvenile sea lamprey. In *A*, lack of banding from two negative controls ([−]Ab and [+]T4) are presented on identically prepared blots alongside positive banding for NKCC1 ([+]T9). In *B*, banding for NKCC1 and HSP90 (~90 kDa) are shown on a single blot containing the membrane (mem) and cytosolic (cyto) fractions of gill homogenates from six individuals acclimated to either FW (1–3) or seawater (SW) (35‰) (4–6). In *D*, representative NKCC1 banding is included above data. Letters depict statistically significant differences [mean ± SE; $n = 3$; one-way ANOVA; Student-Newman-Keuls post hoc (*C*); Dunn's post hoc (*D*)]. RBC, red blood cells.

increased at least 30-fold from larvae (undetected) to migrants ($P < 0.001$; Fig. 5*D*). The first detection of gill NKA and NKCC1 was in stage 6 lamprey, although NKA and NKCC1 could be detected in only 2 of the 8 stage 6 lamprey in our analysis.

In our laboratory comparison between FW-acclimated larvae, and FW- and SW-acclimated postmetamorphic juveniles, gill *nkcc1* was 200-fold higher in FW-acclimated juveniles than in larvae. Gill *nkcc1* increased by ~70% after SW acclimation of juveniles ($P < 0.001$; Fig. 6*A*). Gill NKCC1 protein abundance was at least 25-fold higher in FW-acclimated juveniles than in larvae (undetected) and was ~60% higher in SW-acclimated juveniles compared with FW-acclimated juveniles ($P < 0.001$; Fig. 6*B*). Likewise, juveniles had higher abundances of gill *nka* mRNA ($P < 0.001$; Fig. 6*C*) and NKA protein ($P < 0.001$; Fig. 6*D*) compared with larvae, and SW acclimation significantly increased gill *nka* mRNA and NKA protein. Analysis of the relationship between the relative protein abundances of gill NKA and NKCC1 in FW- and SW-acclimated juveniles revealed a significant correlation ($m = 0.76$, $r^2 = 0.66$, $F_{1,10} = 18.9$, $P < 0.005$; Fig. 7*A*).

Immunohistochemistry of gill NKCC1. T9 immunoreactivity (NKCC1) in the gills of larval sea lamprey was very rarely observed and only ever observed in small cells on the lamellae (Fig. 7*B*). Intense NKCC1 staining was detected in the larger cells in the interlamellar space along the primary filament of postmetamorphic juveniles. A strong fluorescent signal was present throughout the entire body of these cells except for the nucleus, where no NKCC1 staining was present. Very rarely were NKCC1-positive cells observed on the lamellae in juveniles, and the abundance of NKCC1-positive cells on the primary filament was significantly higher in juveniles than in larvae at ~140–150 immunoreactive cells/mm filament length in juveniles. There was no statistical difference in abundance of KNCC1-positive cells between FW- and SW-acclimated juveniles. Results of the two-way ANOVA in Fig. 7*B* were $P_{\text{life-stage}} < 0.001$, $P_{\text{location}} < 0.001$, and $P_{\text{interation}} < 0.001$. NKCC1 colocalized to the same filamental ionocytes as NKA (αRbNKA-immunoreactivity) (Fig. 7*C*).

Pharmacological inhibition of NKCC1. All lamprey were fully recovered (restoration of swimming activity) within 30 min of anesthetization and injection of the NKCC1 inhibitor bumet-
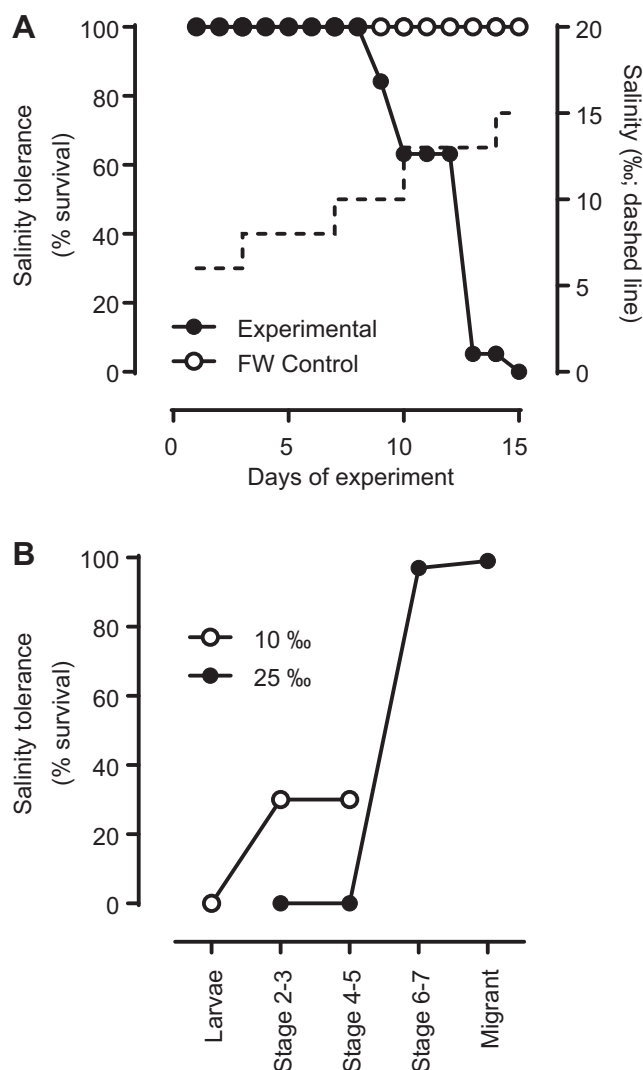
Fig. 4. Salinity tolerance of sea lamprey larvae ($n = 20$) exposed to increasing salinity (*A*) or sea lamprey after direct exposure to elevated salinity (10‰ or 25‰) at various stages throughout metamorphosis (*B*). In *B*, survival rates were assessed 14 days after exposure to elevated salinity and calculated from various salinity trials; $n = 10–20$ (larvae, stage 2–3, stage 4–5) and $n = 60–100$ (stage 6–7, migrant). FW, freshwater.

anide or saline control. In FW lamprey, bumetanide treatment had no effect on plasma Cl^- and osmolality, or muscle water (Fig. 8, *A–C*). Exposure to SW resulted in slight increases in plasma Cl^- and osmolality, and a slight decrease in muscle water content in the VEH control (Fig. 8, *A–C*). Lamprey injected with either 0.1 or 1.0 μmol/g bumetanide and exposed to SW had significantly higher plasma Cl^- (Fig. 8*A*) and plasma osmolality (Fig. 8*B*), and lamprey injected with 1.0 μmol/g had significantly lower muscle water (Fig. 8*C*) compared with the VEH control. Results of the two-way ANOVA were Cl^-: $P_{treatment} = 0.013$, $P_{salinity} < 0.001$, $P_{interaction} < 0.001$; osmolality: $P_{treatment} = 0.038$, $P_{salinity} < 0.001$, $P_{interaction} < 0.001$; muscle water: $P_{treatment} = 0.470$, $P_{salinity} < 0.001$, $P_{interaction} = 0.271$.

DISCUSSION

To the best of our knowledge, prior to this study, no protein-level evidence for the role of NKCC1 in agnathan osmoregulation was available. Here, we have presented the following lines of evidence for the importance of gill NKCC1 in lamprey hypo-osmoregulation: *1*) a tissue profile showing that the gill is the primary site of NKCC1 expression (mRNA and protein abundance), *2*) a metamorphic profile showing substantial increases in gill NKA and NKCC1 expression coinciding with the development of SW tolerance, *3*) further increases in gill NKCC1 and NKA expression after SW acclimation, and *4*) reduced SW tolerance after pharmacological inhibition of NKCC1.

It has been hypothesized that the NKCC1 and NKCC2 isoforms are products of a second whole-genome duplication in the vertebrate lineage (2R), after a prior genome duplication (1R) led to the initial divergence of NKCC from NCC (21), yet whether lampreys radiated after 1R or 2R is still unresolved (25, 42, 60–62). In the present study, we present a full-length peptide sequence of a lamprey NKCC1-like protein. Phylogenetic analysis revealed that the sea lamprey NKCC1 groups strongly with other vertebrate NKCC1 peptides and occupies a basal position in the NKCC1 clade. The sea lamprey NKCC1 displayed a 66% sequence identity to NKCC1 in zebrafish and humans, with only the amino terminus displaying considerable divergence between sea lamprey and zebrafish or humans. This is consistent with the defining structural characteristics of the SLC12A family of cation cotransporters, which includes a highly conserved hydrophobic region (including 12 transmembrane segments) flanked by an N-terminal region with high sequence variability and a highly conserved C-terminal region (45).

In Western blot analysis, the sea lamprey NKCC1 appeared as a single, diffuse band detected primarily in the gill and centered on a molecular mass of ~180 kDa, which is larger than its predicted size of 127 kDa based on peptide sequence alone. However, glycosylation of NKCC1 often leads to higher apparent molecular weights in Western blots. Depending on the species, NKCC1 can appear in Western blotting at sizes ranging from 120 to 130 kDa in its deglycosylated form to 160–220 kDa when glycosylated (35) to over 300 kDa as a homodimer (43). Two of the four predicted *N*-linked glycosylation sites (N504 and N515, Fig. 1) on the large extracellular loop between TM7 and TM8 correspond to the two putative sites of *N*-linked glycosylation on the human NKCC1, which are important in cell surface expression, protein turnover, and Cl^- affinity (44). Thus, it is likely that sea lamprey NKCC1 is a glycoprotein like other vertebrate NKCC1 peptides and that glycosylation explains the higher-than-expected molecular weight of the NKCC1 immunoreactive band observed in Western blotting in the present study.

The T9 antibody used in this study was originally developed by Lytle et al. (35) against a fusion protein of the 310 C-terminal amino acids of the human colonic NKCC1 in the same effort that produced the widely used anti-NKCC1 antibody T4. Originally, the T4 antibody was described as "broadly specific" because of its immunoreactivity with many tissues known to possess NKCC, including NKCC1 in the human colon, shark rectal gland, and duck salt gland, as well as NKCC2 in the mammalian kidney. Since its development, the T4 antibody has been used extensively to detect NKCCs and NCC in a range of fishes, including the teleost gill NKCC1 (48, 67) and NCC (23), the teleost intestinal NKCC2 (8), and the
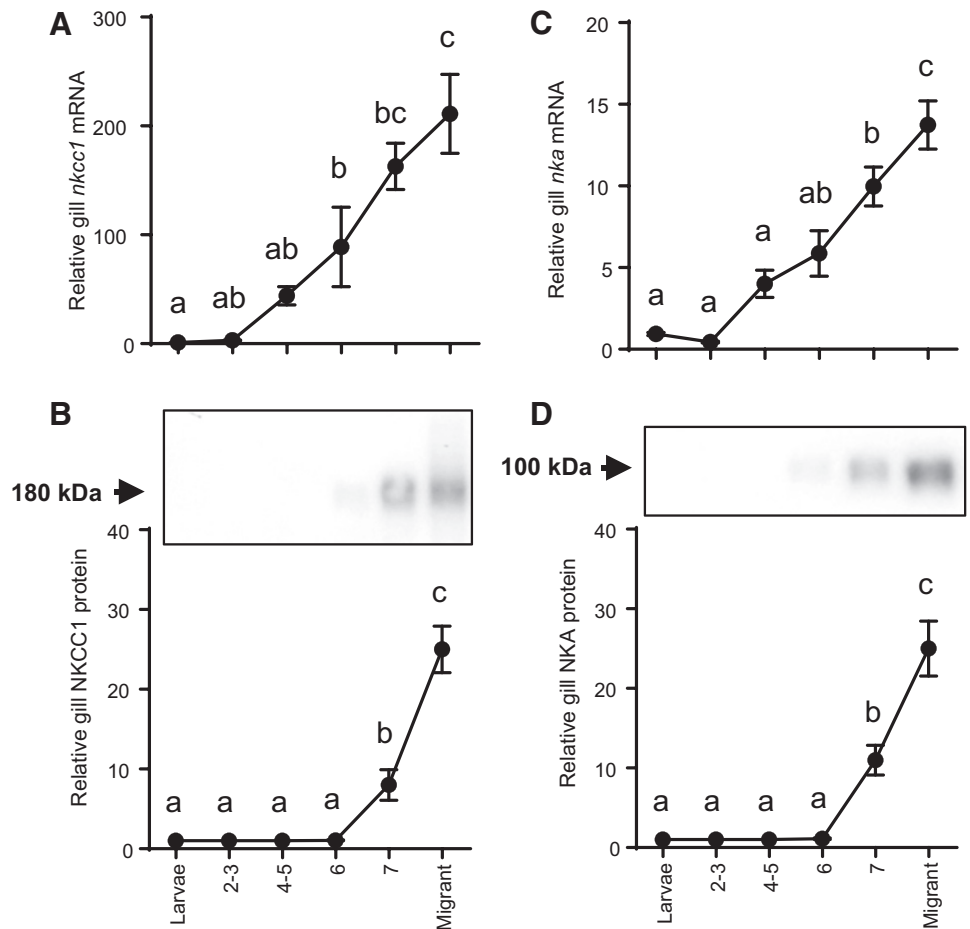
Fig. 5. Metamorphic profile for the relative abundance of Na-K-Cl cotransporter 1 (*nkcc1*) (*A*), NKCC1 (*B*), Na$^+$-K$^+$-ATPase (*nka*) (*C*), and NKA (*D*) in the sea lamprey gill. In *A* and *C* (Student-Newman-Keuls post hoc), data are presented as relative to *ef1α*. In *B* and *D* (Dunn's post hoc), representative T9- and α5-immunoreactive banding is included above respective data. Letters depict statistically significant differences (means ± SE; *n* = 4–10; one-way ANOVA).

sturgeon gill NKCC1 (56, 59). Here, we show that T4 does not immunodetect any NKCC homolog in the lamprey gill. The T9 antibody was also originally produced against the human NKCC1 but described as having "narrow specificity" as it appeared to be immunoreactive with only the mammalian NKCC (both the secretory NKCC1 in the human colon and the absorptive NKCC2 in the mammalian kidney) (35). Since then, T9 has been sparingly used to immunodetect NKCC in published works—once to detect NKCC2 in the rat kidney (1) and once, along with T4, to detect an NKCC homolog in the sea urchin (9). It is not clear why T9 appears to reliably immunodetect the lamprey NKCC1 when it fails to detect NKCC1 in the homologous and, presumably, less evolutionarily distant Cl$^-$-secreting ionocytes of the shark rectal gland, teleost gill, and avian salt gland. The lamprey NKCC1 and human NKCC1 possess only a 62% sequence identity across the 310 C-terminal amino acids against which T9 was raised; however, the sequence identity between the human and lamprey NKCC1 is much higher (76%) when comparing just the 200-most C-terminal amino acids (the more likely site of antigenicity), which may explain how T9 is able to detect the lamprey NKCC1.

Early work in lampreys identified two types of ionocytes on the gill epithelium that were presumed to be specific for either ion uptake or ion secretion (2). After metamorphosis and migration into SW, surface exposure of the ion-secreting ionocytes in the interlamellar space increases and the intercalated cells involved in ion uptake disappear (46, 47). Since then, it

was shown that NKA protein abundance is greater in postmetamorphic juveniles than larvae and that α5 immunoreactivity, which is a widely used marker of ionocytes, shifts from the small cells in the lamellae of larvae to large cells in the filament of juveniles (52). Taken together, these studies indicate that sea lamprey transform the branchial epithelium before SW entry in preparation for hypo-osmoregulation.

We expand on these previous works by resolving the timing of the increase in NKA abundance to the later stages of metamorphosis, describing for the first time the transcriptional upregulation of *nka* and *nkcc1* throughout metamorphosis and colocalizing NKCC1 and NKA to the interlamellar ionocytes along the gill filament. Larvae, which are known to have very low levels of gill NKA abundance and activity (52) and have no detectable NKCC1 (present study), are incapable of surviving in salinities above 10‰. Much like what has been described in the Pacific lamprey (*Entosphenus tridentatus*) (54), we observed the development of SW tolerance in sea lamprey to occur at metamorphic stages 6–7. The major increases in gill NKCC1 and NKA abundance between metamorphic stages 6 and 7 are both preceded by increases in *nkcc1* and *nka* mRNA at earlier stages, potentially illustrating the process of mRNA being translated into protein throughout metamorphosis; it may be that NKCC1 is being expressed in earlier metamorphic stages at levels below our detection limit. The significant and highly correlated upregulation of gill NKCC1 and NKA protein abundance and the development of SW tolerance during
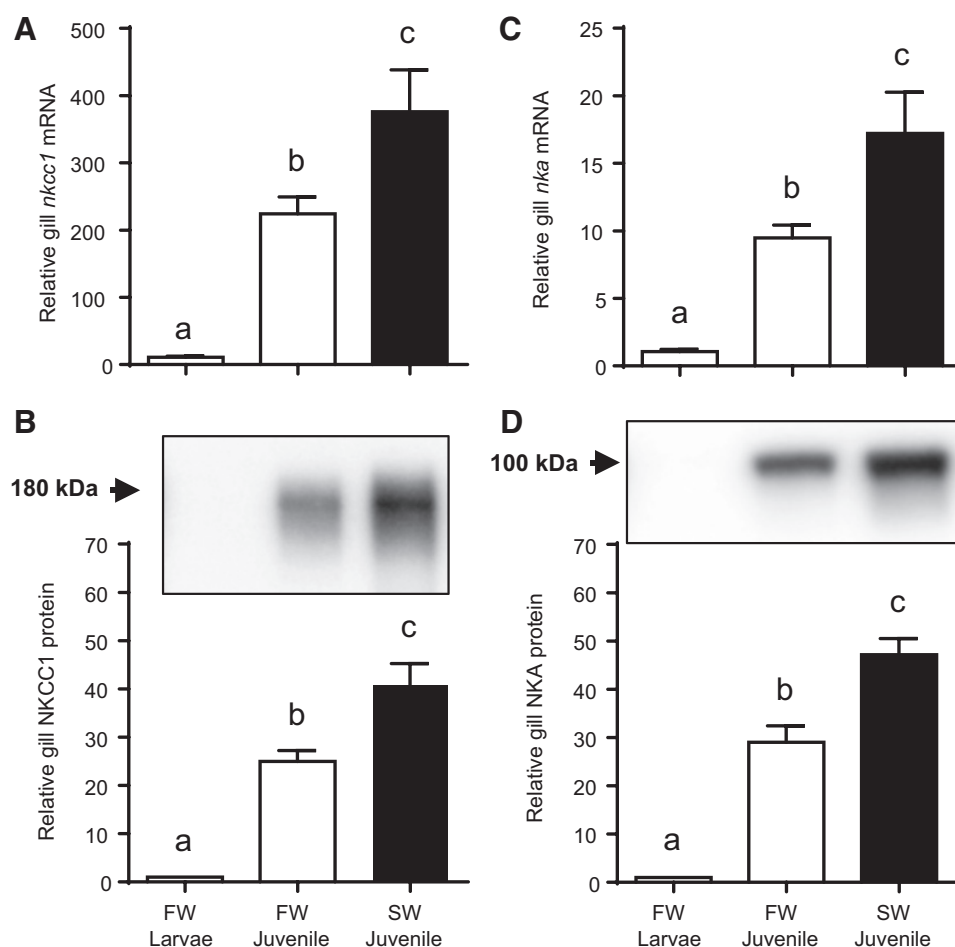
Fig. 6. Relative abundance of Na-K-Cl cotransporter 1 (*nkcc1*) (*A*), NKCC1 (*B*), Na$^+$-K$^+$-ATPase (*nka*) (*C*), and NKA (*D*) in freshwater (FW)-acclimated larvae, FW-acclimated juvenile, and seawater (SW)-acclimated (35‰) juvenile sea lamprey gill. In *A*, the actual value for larvae (1.095 ± 0.18) has been inflated for visual clarity. In *A* and *C* (Student-Newman-Keuls post hoc), data are presented as relative to *ef1α*. In *B* and *D* (Dunn's post hoc), representative T9- and α5-immunoreactive banding is included above respective data. Letters depict statistically significant differences (means ± SE; *n* = 8–10; one-way ANOVA).

metamorphosis provides evidence that branchial ion secretion involves a coupling of NKCC1 and NKA. Acclimation of juvenile lamprey to SW resulted in an additional increase in NKCC1 and NKA, providing further evidence that these ion transporters are critical components of branchial ion secretion in lampreys. This coupling is further supported by the correlation of protein abundance and colocalization of NKCC1 and NKA to the large Cl-secreting ionocytes along the gill filament of postmetamorphic juveniles.

It is interesting that the sea lamprey appears to make many of the hypo-osmoregulatory adjustments before ever entering SW. The elevation of NKA and NKCC1 expression in FW before exposure to SW has also been shown in smolting salmonids (40), which also have a strong correlation between increased levels of these ion transporters and salinity tolerance. It is likely that these proteins and their ionocytes are inactive until exposure to SW, although the mechanism(s) for activation are currently unknown. Trafficking of ion transport proteins to the plasma membrane in response to a physiological challenge has shown to be an important regulatory process in fishes (34, 63); however, this does not appear to be the case for the lamprey NKCC1 in response to SW exposure, based on our observation that NKCC1 is found only in the membrane in the gills of both FW- and SW-acclimated juveniles (Fig. 3). Gill NKCC1 in juvenile sea lamprey exposed to SW may be activated by phosphorylation (16), similarly to what has been shown in mummichog (*Fundulus heteroclitus*) (17). In teleost

fish, inactive ionocytes have been shown to be covered by pavement cells and then rapidly uncovered after SW exposure (8a, 22), and a similar mechanism of ionocyte activation may also be present in sea lamprey.

The hypo-osmoregulatory adjustments made during the sea lamprey metamorphosis are akin to the months-long parr-smolt transformation preceding SW entry that occurs in anadromous salmonids (24, 41). Smolt development and the ontogeny of SW tolerance in salmonids are driven by a coordinated endocrine program involving the stimulatory action of thyroid hormones, cortisol, and growth hormone (40). Lamprey metamorphosis appears to differ from the parr-smolt transformation and most other instances of metamorphosis in vertebrates in that thyroid hormones are antagonistic to transformation, such that the onset of metamorphosis is driven by a sharp decrease in circulating thyroid hormones (72). Lampreys lack the steroidogenic ability to produce cortisol, and so a biosynthetic precursor, 11-deoxycortisol, is presumed to be the putative corticosteroid hormone in lampreys (7, 51). Future work is necessary to identify whether and how thyroid hormones, 11-deoxycortisol, or the lamprey growth hormone (30) regulate the development of SW tolerance and the molecular mechanisms for osmoregulation during the lamprey metamorphosis.

We sought direct evidence for the functional importance of NKCC1 in lamprey ion secretion by pharmacologically inhibiting NKCC1 with the widely used NKCC inhibitor bumetanide and subsequently assessing multiple osmoregulatory end
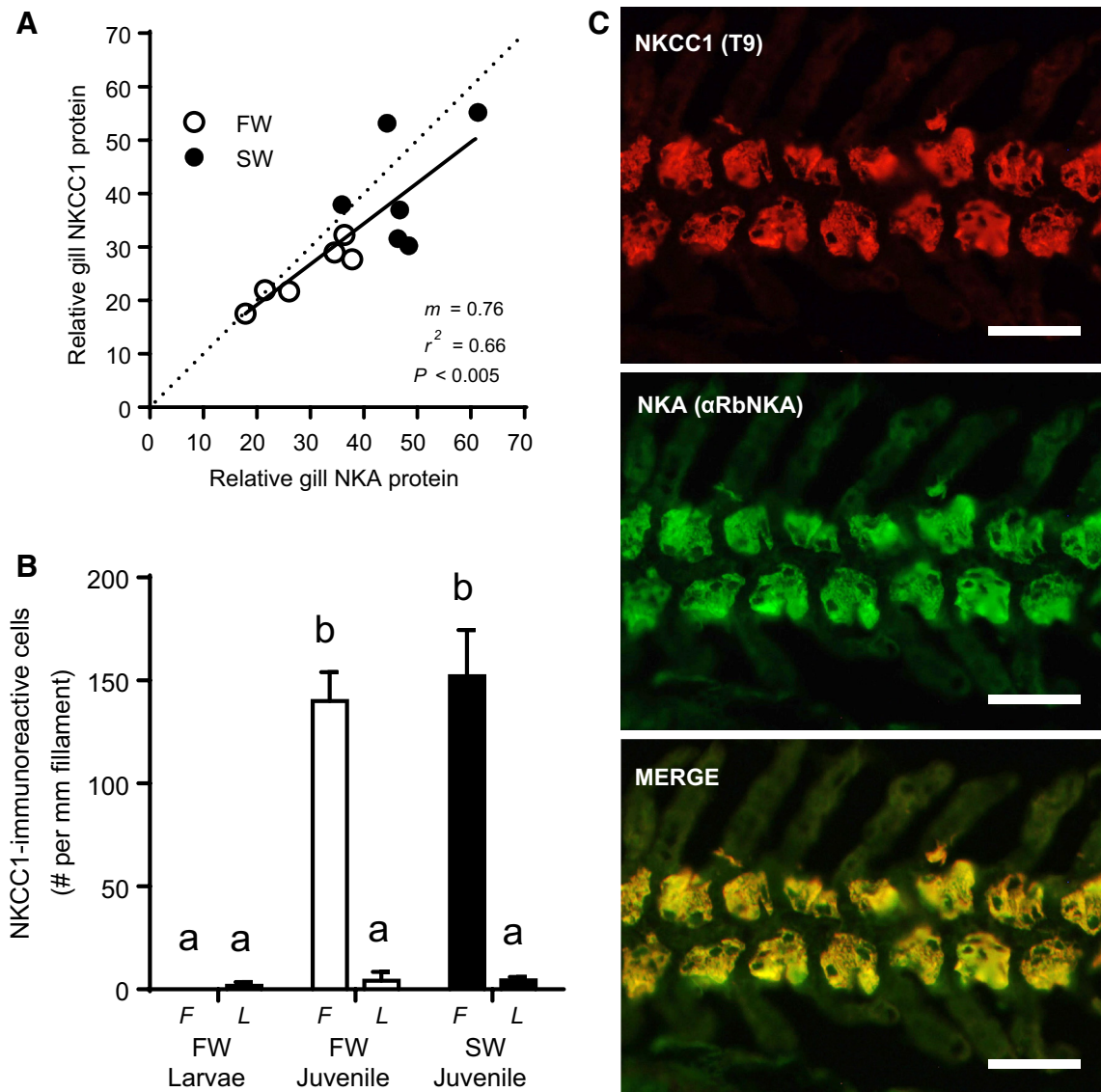
Fig. 7. Relationship between $Na^+-K^+-ATPase$ (NKA) and Na-K-Cl cotransporter 1 (NKCC1) protein abundance (from Western blotting) in freshwater (FW)- and seawater (SW)-acclimated juveniles (*A*), abundance of NKCC1-immunoreactive cells on the primary filament (F) and secondary lamellae (L) of larvae, FW-, and SW-acclimated juveniles (*B*), and representative images of anti-NKCC1 (red) and anti-NKA immunoreactivity (green) in sagittally sectioned (5 μm) gill tissue of SW-acclimated (35‰) juvenile sea lamprey (*C*). In *C*, scale bar = 50 μm. Letters depict statistically significant differences (means ± SE; *n* = 5; two-way ANOVA; Dunn's post hoc).

points. Here, we show that treatment with bumetanide compromises the capacity for juvenile sea lamprey to maintain ion and water homeostasis after exposure to SW. Application of "loop" diuretic compounds, such as bumetanide or furosemide, to ion-transporting epithelia has been classically performed to identify the involvement in NKCC in Cl^- transport (20). This pharmacological approach typically employs in vitro electrophysiological techniques, such as patch clamp or Ussing chamber preparations, that require uniform epithelial tissue, such as the intestine, gill operculum, or culture-raised epithelia. Unfortunately, these techniques cannot be applied to the highly irregular morphology of the fish gill. Thus, our in vivo approach follows several studies using in vivo bumetanide administration in mammals (5, 11, 12, 27, 28, 39, 57, 64) as well as a previous study in fish (50), in which a known NKCC inhibitor, furosemide, was administered by intraperitoneal in-

jection and osmoregulatory targets, such as plasma ion concentration and muscle moisture, were analyzed. The obvious disadvantage of this approach is that the gill is not an isolated target of bumetanide and thus inhibition of NKCC1 or NKCC2 in other tissues could be contributing to the loss of osmoregulatory capacity in SW. We address the potential limitations of this in vivo approach with the following considerations: *1*) our transcriptional- and protein-level data indicate that NKCC1 abundance is far greater in the gill than any other tissue, and thus any NKCC1 inhibition by bumetanide treatment is likely occurring primarily in the gill, *2*) bumetanide application to ex vivo intestinal preparations of SW-acclimated postmetamorphic juvenile sea lamprey does not affect ion uptake as measured by short-circuit current (A. Barany-Ruiz, Universidad de Cádiz, Spain; oral communication), and *3*) analysis of the Japanese and sea lamprey genomes and the hagfish genomes
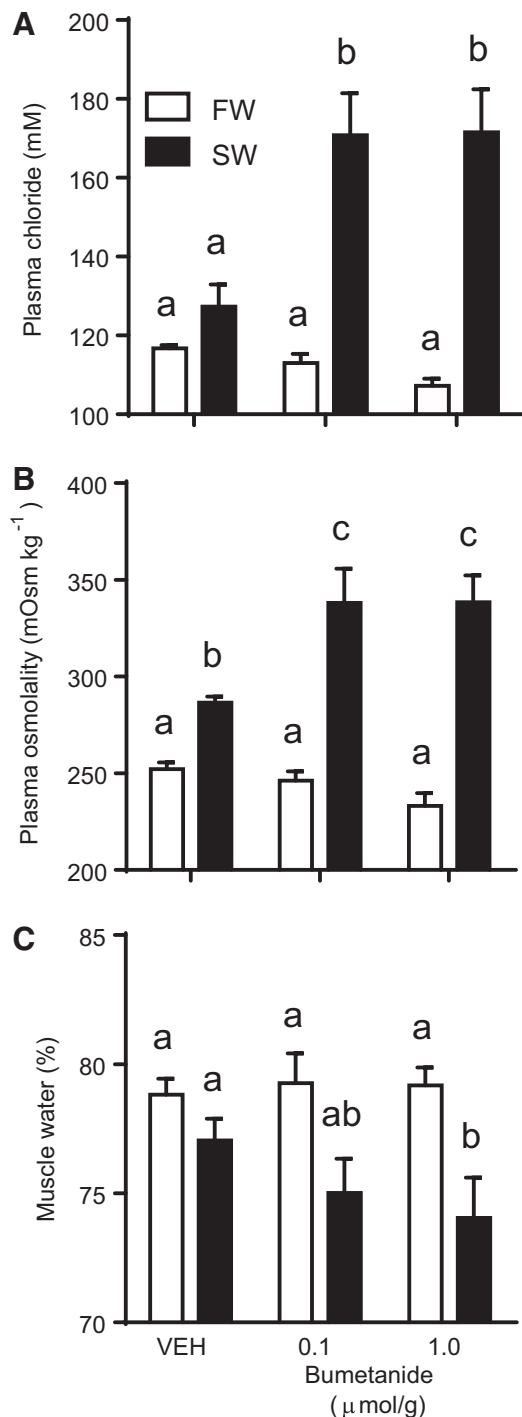
Fig. 8. Effect of intraperitoneal injection of bumetanide [an Na-K-Cl cotransporter 1 (NKCC1) inhibitor] on plasma chloride (*A*), plasma osmolality (*B*), and muscle water (*C*) of sea lamprey compared with a vehicle (VEH) control. After bumetanide injection, fish were exposed to seawater (SW) (35‰, black bars) or freshwater (FW) (white bars) for 24 h. Letters depict statistically significant differences (means ± SE; $n = 8–10$, two-way ANOVA; Student-Newman-Keuls post hoc).

have failed to identify a gene encoding NKCC2. Although the inability to detect a gene in a genome must be viewed with some caution, the apparent lack of an NKCC2 in the genomes of these basal vertebrates could indicate that a duplication of NKCC occurred after the divergence of agnathans from other vertebrates or that NKCC2 has been lost in agnathans. Taken together, the evidence available to us supports that our in vivo approach presented here to inhibit the NKCC1 using bumetanide is likely acting in large proportion on gill NKCC1, thus providing evidence for the functional importance of branchial NKCC1 in ion and water balance of SW lamprey.

Although the role of NKCC1 in transcellular Cl^- secretion in the gills of marine fishes is widely accepted (14, 26) and such a role has been proposed in lampreys (2), the present study offers the first protein level and functional evidence for the role of NKCC1 in lampreys. The robust upregulation of basolateral NKA and NKCC1 during metamorphosis in the anadromous sea lamprey may be a good biomarker for distinguishing anadromous sea lamprey from landlocked strains or anadromous lamprey species from their riverine species pairs. Still unresolved is the apical pathway for Cl^- to exit the sea lamprey ionocyte, which in later-evolved fish lineages is the CFTR (38). Although the gene encoding the lamprey CFTR has been cloned (53), an RNAseq approach from the same study revealed relatively low *cftr* mRNA transcript abundance in all tissues, including the adult gill, with the only exception being high expression in the larval intestine. Further research is needed to establish the apical pathway of Cl^- secretion in lampreys to complete the molecular characterization of this basal vertebrate ionocyte.

In conclusion, the present study provides a molecular and functional characterization of the sea lamprey NKCC1. We show that gill NKCC1 expression (mRNA and protein abundance) increases dramatically during metamorphosis, coinciding with the development of SW tolerance, and that NKCC1 expression increases further after SW acclimation. Immunoblotting and immunohistochemical analyses colocalized NKCC1 with NKA to the plasma membrane fraction of the presumptive Cl^- secreting gill ionocytes along the filament. Finally, we demonstrated a functional role for NKCC1 in hypo-osmoregulation by showing that pharmacological inhibition of NKCC1 in postmetamorphic juveniles results in reduced SW tolerance.

Perspectives and Significance

The present study provides evidence that the basolateral pathway for ion secretion across the lamprey gill involves a coupling of NKCC1 and NKA in branchial ionocytes, moving back the most basal example of a role of NKCC1 in salt secretion in vertebrates by ~100 million years from Chondrichthyes (sharks), which first appeared as early as 450 million years ago, to Agnathans (lamprey), which first appeared over 550 million years ago. This work is a part of many recent advances in lamprey physiology (osmoregulation, endocrinology, immunology, and neurobiology) and genetics (publication and updating of the lamprey genome), which have combined to establish lamprey as an important model system for the study of vertebrate evolution. Although our work here demonstrates that the role of a basolateral NKCC1 in a secretory epithelium is ancestral among vertebrates, we also underscore a need for further investigation into still unresolved ionoregulatory processes in lamprey and the endocrine pathways that control them.

REFERENCES

1. **Alvarez de la Rosa D, Coric T, Todorovic N, Shao D, Wang T, Canessa CM.** Distribution and regulation of expression of serum- and glucocorticoid-induced kinase-1 in the rat kidney. *J Physiol* 551: 455–466, 2003. doi:10.1113/jphysiol.2003.042903.

2. **Bartels H, Potter IC.** Cellular composition and ultrastructure of the gill epithelium of larval and adult lampreys: implications for osmoregulation in fresh and seawater. *J Exp Biol* 207: 3447–3462, 2004. doi:10.1242/jeb.01157.

3. **Beamish FWH.** Biology of the North American anadromous sea lamprey, Petromyzon marinus. *Can J Fish Aquat Sci* 37: 1924–1943, 1980. doi:10.1139/f80-233.

4. **Beamish FWH.** Osmoregulation in juvenile and adult lampreys. *Can J Fish Aquat Sci* 37: 1739–1750, 1980. doi:10.1139/f80-219.

5. **Ben-Ari Y, Cherubini E, Corradetti R, Gaiarsa J-L.** Giant synaptic potentials in immature rat CA3 hippocampal neurones. *J Physiol* 416: 303–325, 1989. doi:10.1113/jphysiol.1989.sp017762.

6. **Bradley TJ.** *Animal osmoregulation.* New York: Oxford University Press, 2009.

7. **Close DA, Yun S-S, McCormick SD, Wildbill AJ, Li W.** 11-Deoxycortisol is a corticosteroid hormone in the lamprey. *Proc Natl Acad Sci USA* 107: 13,942–13,947, 2010. doi:10.1073/pnas.0914026107.

8. **Cutler CP, Cramb G.** Two isoforms of the Na+/K+/2Cl- cotransporter are expressed in the European eel (Anguilla anguilla). *Biochim Biophys Acta* 1566: 92–103, 2002. doi:10.1016/S0005-2736(02)00596-5.

8a. **Daborn K, Cozzi RRF, Marshall WS.** Dynamics of pavement cell-chloride cell interactions during abrupt salinity change in *Fundulus heteroclitus. J Exp Biol* 204: 1889–1899, 2001.

9. **D'Andrea-Winslow L, Strohmeier GR, Rossi B, Hofman P.** Identification of a sea urchin Na(+)/K(+)/2Cl(-) cotransporter (NKCC): microfilament-dependent surface expression is mediated by hypotonic shock and cyclic AMP. *J Exp Biol* 204: 147–156, 2001.

11. **Dzhala VI, Brumback AC, Staley KJ.** Bumetanide enhances phenobarbital efficacy in a neonatal seizure model. *Ann Neurol* 63: 222–235, 2008. doi:10.1002/ana.21229.

12. **Dzhala VI, Talos DM, Sdrulla DA, Brumback AC, Mathews GC, Benke TA, Delpire E, Jensen FE, Staley KJ.** NKCC1 transporter facilitates seizures in the developing brain. *Nat Med* 11: 1205–1213, 2005. doi:10.1038/nm1301.

13. **Esbaugh AJ, Cutler B.** Intestinal Na$^+$, K$^+$, 2Cl$^-$ cotransporter 2 plays a crucial role in hyperosmotic transitions of a euryhaline teleost. *Physiol Rep* 4: e13028, 2016. doi:10.14814/phy2.13028.

14. **Evans DH.** Teleost fish osmoregulation: what have we learned since August Krogh, Homer Smith, and Ancel Keys. *Am J Physiol Regul Integr Comp Physiol* 295: R704–R713, 2008. doi:10.1152/ajpregu.90337.2008.

15. **Ferreira-Martins D, Coimbra J, Antunes C, Wilson JM.** Effects of salinity on upstream-migrating, spawning sea lamprey, Petromyzon marinus. *Conserv Physiol* 4: cov064, 2016. doi:10.1093/conphys/cov064.

16. **Flatman PW.** Regulation of Na-K-2Cl cotransport by phosphorylation and protein-protein interactions. *Biochim Biophys Acta* 1566: 140–151, 2002. doi:10.1016/s0005-2736(02)00586-2.

17. **Flemmer AW, Monette MY, Djurisic M, Dowd B, Darman R, Gimenez I, Forbush B.** Phosphorylation state of the Na+-K+-Cl- cotransporter (NKCC1) in the gills of Atlantic killifish (Fundulus heteroclitus) during acclimation to water of varying salinity. *J Exp Biol* 213: 1558–1566, 2010. doi:10.1242/jeb.039644.

18. **Geck P, Pietrzyk C, Burckhardt B-C, Pfeiffer B, Heinz E.** Electrically silent cotransport on Na+, K+ and Cl- in Ehrlich cells. *Biochim Biophys Acta* 600: 432–447, 1980. doi:10.1016/0005-2736(80)90446-0.

19. **Haas M, Forbush B III.** The Na-K-Cl cotransporters. *J Bioenerg Biomembr* 30: 161–172, 1998. doi:10.1023/A:1020521308985.

20. **Haas M, Forbush B III.** The Na-K-Cl cotransporter of secretory epithelia. *Annu Rev Physiol* 62: 515–534, 2000. doi:10.1146/annurev.physiol.62.1.515.

21. **Hartmann AM, Tesch D, Nothwang HG, Bininda-Emonds ORP.** Evolution of the cation chloride cotransporter family: ancient origins, gene losses, and subfunctionalization through duplication. *Mol Biol Evol* 31: 434–447, 2014. doi:10.1093/molbev/mst225.

22. **Heijden A, Verbost P, Eygensteyn J, Li J, Bonga S, Flik G.** Mitochondria-rich cells in gills of tilapia (*Oreochromis mossambicus*) adapted to fresh water or sea water: quantification by confocal laser scanning microscopy. *J Exp Biol* 200: 55–64, 1997.

23. **Hiroi J, Yasumasu S, McCormick SD, Hwang P-P, Kaneko T.** Evidence for an apical Na-Cl cotransporter involved in ion uptake in a teleost fish. *J Exp Biol* 211: 2584–2599, 2008. doi:10.1242/jeb.018663.

24. **Hoar WS.** The physiology of smolting salmonids. In: *Fish Physiology*, edited by Hoar WS, Randall DJ. San Diego, CA: Academic, p. 275–343.

25. **Holland LZ, Ocampo Daza D.** A new look at an old question: when did the second whole genome duplication occur in vertebrate evolution? *Genome Biol* 19: 209, 2018. doi:10.1186/s13059-018-1592-0.

26. **Hwang PP, Lee TH, Lin LY.** Ion regulation in fish gills: recent progress in the cellular and molecular mechanisms. *Am J Physiol Regul Integr Comp Physiol* 301: R28–R47, 2011. doi:10.1152/ajpregu.00047.2011.

27. **Javaheri S, Wagner KR.** Bumetanide decreases canine cerebrospinal fluid production. In vivo evidence for NaCl cotransport in the central nervous system. *J Clin Invest* 92: 2257–2261, 1993. doi:10.1172/JCI116829.

28. **Kahle KT, Barnett SM, Sassower KC, Staley KJ.** Decreased seizure activity in a human neonate treated with bumetanide, an inhibitor of the Na(+)-K(+)-2Cl(-) cotransporter NKCC1. *J Child Neurol* 24: 572–576, 2009. doi:10.1177/0883073809333526.

29. **Kahle KT, Staley KJ, Nahed BV, Gamba G, Hebert SC, Lifton RP, Mount DB.** Roles of the cation-chloride cotransporters in neurological disease. *Nat Clin Pract Neurol* 4: 490–503, 2008. doi:10.1038/ncpneuro0883.

30. **Kawauchi H, Suzuki K, Yamazaki T, Moriyama S, Nozaki M, Yamaguchi K, Takahashi A, Youson J, Sower SA.** Identification of growth hormone in the sea lamprey, an extant representative of a group of the most ancient vertebrates. *Endocrinology* 143: 4916–4921, 2002. doi:10.1210/en.2002-220810.

31. **Kolosov D, Bui P, Donini A, Wilkie MP, Kelly SP.** A role for tight junction-associated MARVEL proteins in larval sea lamprey (*Petromyzon marinus*) osmoregulation. *J Exp Biol* 220: 3657–3670, 2017. doi:10.1242/jeb.161562.

32. **Kumar S, Stecher G, Tamura K.** MEGA7: molecular evolutionary genetics analysis version 7.0 for bigger datasets. *Mol Biol Evol* 33: 1870–1874, 2016. doi:10.1093/molbev/msw054.

33. **Lambert IH, Hoffmann EK, Pedersen SF.** Cell volume regulation: physiology and pathophysiology. *Acta Physiol (Oxf)* 194: 255–282, 2008. doi:10.1111/j.1748-1716.2008.01910.x.

34. **Lingwood D, Harauz G, Ballantyne JS.** Regulation of fish gill Na(+)-K(+)-ATPase by selective sulfatide-enriched raft partitioning during seawater adaptation. *J Biol Chem* 280: 36545–36550, 2005. doi:10.1074/jbc.M506670200.

35. **Lytle C, Xu J-CC, Biemesderfer D, Forbush B III.** Distribution and diversity of Na-K-Cl cotransport proteins: a study with monoclonal antibodies. *Am J Physiol Cell Physiol* 269: C1496–C1505, 1995. doi:10.1152/ajpcell.1995.269.6.C1496.

36. **Lytle C, Xu JC, Biemesderfer D, Haas M, Forbush B III.** The Na-K-Cl cotransport protein of shark rectal gland. I. Development of monoclonal antibodies, immunoaffinity purification, and partial biochemical characterization. *J Biol Chem* 267: 25428–25437, 1992.

37. **Marshall WS, Grosell M.** Ion transport, osmoregulation, and acid-base balance. In: *The Physiology of Fishes*, edited by Evans DH, Claiborne JB. Boca Raton, FL: Taylor and Francis Group, 2006, p. 177–230.

38. **Marshall WS, Singer TD.** Cystic fibrosis transmembrane conductance regulator in teleost fish. *Biochim Biophys Acta* 1566: 16–27, 2002. doi:10.1016/S0005-2736(02)00584-9.

39. **Mazarati A, Shin D, Sankar R.** Bumetanide inhibits rapid kindling in neonatal rats. *Epilepsia* 50: 2117–2122, 2009. doi:10.1111/j.1528-1167.2009.02048.x.

40. **McCormick SD.** Smolt physiology and endocrinology. In: *Fish Physiology: Euryhaline Fishes*, edited by McCormick SD, Farrell AP, Brauner CJ. Amsterdam: Academic, 2013, p. 191–251.

41. **McCormick SD, Saunders RL.** Preparatory physiological adaptations for marine life of salmonids: osmoregulation, growth, and metabolism. *Am Fish Soc Symp* 1: 211–229, 1987.

42. **Mehta TK, Ravi V, Yamasaki S, Lee AP, Lian MM, Tay B-H, Tohari S, Yanai S, Tay A, Brenner S, Venkatesh B.** Evidence for at least six Hox clusters in the Japanese lamprey (Lethenteron japonicum). *Proc Natl Acad Sci USA* 110: 16044–16049, 2013. doi:10.1073/pnas.1315760110.

43. **Moore-Hoon ML, Turner RJ.** The structural unit of the secretory Na$^+$-K$^+$-2Cl$^-$ cotransporter (NKCC1) is a homodimer. *Biochemistry* 39: 3718–3724, 2000. doi:10.1021/bi992301v.

44. **Paredes A, Plata C, Rivera M, Moreno E, Vázquez N, Muñoz-Clares R, Hebert SC, Gamba G.** Activity of the renal Na$^+$-K$^+$-2Cl$^-$ cotransporter is reduced by mutagenesis of N-glycosylation sites: role for protein surface charge in Cl- transport. *Am J Physiol Renal Physiol* 290: F1094–F1102, 2006. doi:10.1152/ajprenal.00071.2005.

45. **Payne JA, Forbush B III.** Molecular characterization of the epithelial Na-K-Cl cotransporter isoforms. *Curr Opin Cell Biol* 7: 493–503, 1995. doi:10.1016/0955-0674(95)80005-0.

46. **Peek WD, Youson JH.** Ultrastructure of chloride cells in young adults of the anadromous sea lamprey, *Petromyzon marinus L.*, in fresh water and during adaptation to sea water. *J Morphol* 160: 143–163, 1979. doi:10.1002/jmor.1051600203.

47. **Peek WD, Youson JH.** Transformation of the interlamellar epithelium of the gills of the anadromous sea lamprey, *Petromyzon marinus* L., during metamorphosis. *Can J Zool* 57: 1318–1332, 1979. doi:10.1139/z79-168.

48. **Pelis RM, Zydlewski J, McCormick SD.** Gill Na$^+$-K$^+$-2Cl$^-$ cotransporter abundance and location in Atlantic salmon: effects of seawater and smolting [Online]. *Am J Physiol Regul Integr Comp Physiol* 280: R1844–R1852, 2001. doi:10.1152/ajpregu.2001.280.6.R1844.

49. **Potter IC, Beamish FWH.** The freshwater biology of adult anadromous sea lampreys Petromyzon marinus. *J Zool* 181: 113–130, 1977. doi:10.1111/j.1469-7998.1977.tb04573.x.

50. **Prodocimo V, Freire CA.** The Na$^+$-K$^+$-2Cl$^-$ cotransporter of estuarine pufferfishes (Sphoeroides testudineus and S. greeleyi) in hypo- and hyper-regulation of plasma osmolality. *Comp Biochem Physiol C Toxicol Pharmacol* 142: 347–355, 2006. doi:10.1016/j.cbpc.2005.11.013.

51. **Rai S, Szeitz A, Roberts BW, Christie Q, Didier W, Eom J, Yun SS, Close DA.** A putative corticosteroid hormone in Pacific lamprey, *Entosphenus tridentatus*. *Gen Comp Endocrinol* 212: 178–184, 2015. doi:10.1016/j.ygcen.2014.06.019.

52. **Reis-Santos P, McCormick SD, Wilson JM.** Ionoregulatory changes during metamorphosis and salinity exposure of juvenile sea lamprey (*Petromyzon marinus* L.). *J Exp Biol* 211: 978–988, 2008. doi:10.1242/jeb.014423.

53. **Ren J, Chung-Davidson Y-W, Yeh C-Y, Scott C, Brown T, Li W.** Genome-wide analysis of the ATP-binding cassette (ABC) transporter gene family in sea lamprey and Japanese lamprey. *BMC Genomics* 16: 436, 2015. doi:10.1186/s12864-015-1677-z.

54. **Richards JE, Beamish FWH.** Initiation of feeding and salinity tolerance in the pacific *lamprey Lampetra tridentata*. *Mar Biol* 63: 73–77, 1981. doi:10.1007/BF00394664.

55. **Russell JM.** Sodium-potassium-chloride cotransport. *Physiol Rev* 80: 211–276, 2000. doi:10.1152/physrev.2000.80.1.211.

56. **Sardella BA, Kültz D.** Osmo- and ionoregulatory responses of green sturgeon (*Acipenser medirostris*) to salinity acclimation. *J Comp Physiol B* 179: 383–390, 2009. doi:10.1007/s00360-008-0321-5.

57. **Sipilä ST, Schuchmann S, Voipio J, Yamada J, Kaila K.** The cation-chloride cotransporter NKCC1 promotes sharp waves in the neonatal rat hippocampus. *J Physiol* 573: 765–773, 2006. doi:10.1113/jphysiol.2006.107086.

58. **Shankar SS, Brater DC.** Loop diuretics: from the Na-K-2Cl transporter to clinical use. *Am J Physiol Renal Physiol* 284: F11–F21, 2003. doi:10.1152/ajprenal.00119.2002.

59. **Shaughnessy CA, Baker DW, Brauner CJ, Morgan JD, Bystriansky JS.** Interaction of osmoregulatory and acid-base compensation in white sturgeon (*Acipenser transmontanus*) during exposure to aquatic hypercarbia and elevated salinity [Online]. [abstract]. *J Exp Biol* 218: 2712–2719, 2015. doi:10.1242/jeb.125567.

60. **Smith JJ, Keinath MC.** The sea lamprey meiotic map improves resolution of ancient vertebrate genome duplications. *Genome Res* 25: 1081–1090, 2015. doi:10.1101/gr.184135.114.

61. **Smith JJ, Kuraku S, Holt C, Sauka-Spengler T, Jiang N, Campbell MS, Yandell MD, Manousaki T, Meyer A, Bloom OE, Morgan JR, Buxbaum JD, Sachidanandam R, Sims C, Garruss AS, Cook M, Krumlauf R, Wiedemann LM, Sower SA, Decatur WA, Hall JA, Amemiya CT, Saha NR, Buckley KM, Rast JP, Das S, Hirano M, McCurley N, Guo P, Rohner N, Tabin CJ, Piccinelli P, Elgar G, Ruffier M, Aken BL, Searle SM, Muffato M, Pignatelli M, Herrero J, Jones M, Brown CT, Chung-Davidson YW, Nanlohy KG, Libants SV, Yeh CY, McCauley DW, Langeland JA, Pancer Z, Fritzsch B, de Jong PJ, Zhu B, Fulton LL, Theising B, Flicek P, Bronner ME, Warren WC, Clifton SW, Wilson RK, Li W.** Sequencing of the sea lamprey (*Petromyzon marinus*) genome provides insights into vertebrate evolution. *Nat Genet* 45: 415–421, 2013. doi:10.1038/ng.2568.

62. **Smith JJ, Timoshevskaya N, Ye C, Holt C, Keinath MC, Parker HJ, Cook ME, Hess JE, Narum SR, Lamanna F, Kaessmann H, Timoshevskiy VA, Waterbury CKM, Saraceno C, Wiedemann LM, Robb SMC, Baker C, Eichler EE, Hockman D, Sauka-Spengler T, Yandell M, Krumlauf R, Elgar G, Amemiya CT.** The sea lamprey germline genome provides insights into programmed genome rearrangement and vertebrate evolution. *Nat Genet* 50: 270–277, 2018. [Erratum in Nat Genet. 50: 768, 2018.] doi:10.1038/s41588-017-0036-1.

63. **Tresguerres M, Parks SK, Katoh F, Goss GG.** Microtubule-dependent relocation of branchial V-H+-ATPase to the basolateral membrane in the Pacific spiny dogfish (Squalus acanthias): a role in base secretion. *J Exp Biol* 209: 599–609, 2006. doi:10.1242/jeb.02059.

64. **Wang S, Zhang XQ, Song CG, Xiao T, Zhao M, Zhu G, Zhao CS.** In vivo effects of bumetanide at brain concentrations incompatible with NKCC1 inhibition on newborn DGC structure and spontaneous EEG seizures following hypoxia-induced neonatal seizures. *Neuroscience* 286: 203–215, 2015. doi:10.1016/j.neuroscience.2014.11.031.

65. **Wiley JS, Cooper RA.** A furosemide-sensitive cotransport of sodium plus potassium in the human red cell. *J Clin Invest* 53: 745–755, 1974. doi:10.1172/JCI107613.

66. **Wilson JM, Leitão A, Gonçalves AF, Ferreira C, Fonseca PR, Fonseca A, da Silva JM, Antunes JC, Pereira-Wilson C, Coimbra J.** Modulation of branchial ion transport protein expression by salinity in glass eels (*Anguilla anguilla* L.). *Mar Biol* 151: 1633–1645, 2007. doi:10.1007/s00227-006-0579-7.

67. **Wilson JM, Randall DJ, Donowitz M, Vogl AW, Ip AK.** Immunolocalization of ion-transport proteins to branchial epithelium mitochondria-rich cells in the mudskipper (*Periophthalmodon schlosseri*). *J Exp Biol* 203: 2297–2310, 2000.

68. **Xu J-C, Lytle C, Zhu TT, Payne JA, Benz E Jr, Forbush B III.** Molecular cloning and functional expression of the bumetanide-sensitive Na-K-Cl cotransporter. *Proc Natl Acad Sci USA* 91: 2201–2205, 1994. doi:10.1073/pnas.91.6.2201.

69. **Xue H, Liu S, Ji T, Ren W, Zhang XH, Zheng LF, Wood JD, Zhu JX.** Expression of NKCC2 in the rat gastrointestinal tract. *Neurogastroenterol Motil* 21: 1068–e89, 2009. doi:10.1111/j.1365-2982.2009.01334.x.

70. **Youson JH, Potter IC.** A description of the stages in the metamorphosis of the anadromous sea lamprey, L. *Can J Zool* 57: 1808–1817, 1979. doi:10.1139/z79-235.

71. **Youson JH.** Morphology and physiology of lamprey metamorphosis. *Can J Fish Aquat Sci* 37: 1687–1710, 1980. doi:10.1139/f80-216.

72. **Youson JH.** Is lamprey metamorphosis regulated by thyroid hormones? *Am Zool* 37: 441–460, 1997. doi:10.1093/icb/37.6.441.

73. **Youson JH.** The biology of metamorphosis in sea lampreys: endocrine, environmental, and physiological cues and events, and their potential application to lamprey control. *J Great Lakes Res* 29: 26–49, 2003. doi:10.1016/S0380-1330(03)70476-6.